

# Sustainable Detection and Monitoring of Psychiatric Risk and Abnormal Behavioral States using Multimodal Biosensor Data

Akshaya D. Shetty<sup>1</sup>, Usha Desai<sup>2\*</sup>, Akash Saxena<sup>3</sup>

<sup>1,2</sup>Department of Electronics and Communication Engineering, S.E.A College of Engineering & Technology, Bengaluru, Karnataka, India.

<sup>1</sup>Department of Artificial Intelligence and Machine Learning, Vivekananda College of Engineering & Technology, Puttur, Karnataka, India.

<sup>1,2</sup>Visvesvaraya Technological University, Belagavi, Karnataka, India.

<sup>3</sup>Department of Electrical Engineering, School of Engineering and Technology, Central University of Haryana, Haryana, India.

**E-mail:** <sup>1</sup>akshaya926@gmail.com, <sup>2\*</sup>dr.ushadesai@seaedu.ac.in, <sup>3</sup>drakash@cuh.ac.in

**Orcid ID:** <sup>2\*</sup>0000-0002-2267-2567

## Abstract

Subjects exhibiting neurological, developmental, and behavioral disorders can manifest stress, agitation, and emotional deregulation. The prolonged emotional deregulation increases the development of depression, anxiety disorders and in extreme cases, this persistent deregulation contributes to onset of psychiatric symptoms. This study proposes a novel approach for the detection of psychiatric risk and abnormal behavioral states using multimodal biosensors integration namely Pulse, Electromyography (EMG), and Galvanic Skin Response (GSR) sensors. This experiment was conducted in a skill-training centre for Endosulfan victims aged  $13 \pm 2$  years with the necessary care and consent. Significant differences in electro-dermal signals such as GSR, pulse, and EMG were observed among 66 subjects, with multiple trials conducted for each subject, resulting in a dataset comprising 793 healthy and 750 high risk samples, respectively. Data acquisition was performed by integrating sensors onto the Arduino UNO microcontroller and the Cool-Term software tool. In total, fifteen nonlinear transform domain features were extracted. The confidence intervals of the features were verified using the t-test ( $p < 0.05$ ). A classification model was created using machine learning algorithms, namely Logistic Regression, Random Forest, Gradient Boosting, Support Vector Machine (SVM), K-Nearest Neighbors (KNN), XGBoost, and Neural Networks. Among these, Random Forest, XGBoost, and Neural Networks achieved a sustainable accuracy of 97.92%, while the ensemble model achieved an accuracy of 98.32%. This approach of biosensor monitoring helps to consistently predict the behavioral states of differently abled individuals and supports healthcare providers in the early identification of behavioral and physiological markers indicative of psychiatric risks, contributing to a sustainable mental health ecosystem.

**Keywords:** Electrodermal Activity, Skin Conductance, Galvanic Skin Response (GSR), Biofeedback, Endosulfan Disabled Individuals, Kernel Density Estimation (KDE).

\* Corresponding Author

Journal of Innovative Image Processing, March 2026, Volume 8, Issue 1, Pages 415-438

DOI: <https://doi.org/10.36548/jiip.2026.1.022>

Received: 02.02.2026, received in revised form: 28.02.2026, accepted: 13.03.2026, published: 25.03.2026

© 2026 Inventive Research Organization. This is an open access article under the Creative Commons Attribution 4.0 International (CC BY 4.0) License

## 1. Introduction

The World Health Organization (WHO) reports that mental health distress affects one in 300 individuals globally [1], primarily impacting the adult population. Psychotic behaviour is a symptom of schizophrenia, where a behavioral state reflects the strength of emotional arousal using the Galvanic Skin Response (GSR). GSR extracts psychophysiological patterns, the response system is known as Electro-Dermal Activity (EDA), formerly referred to as GSR. The variations in emotional arousal are measured using GSR on the surface of the skin through the parameter of electrical conductance. This non-invasive technique is crucial in evaluating psychological states, signifying an individual's expressively charged situations, such as being frightened or excited. The level of emotional arousal fluctuates and is classified as negative (such as "threatening" or "saddening") or positive (such as "happy" or "joyful"). Nevertheless, the current GSR signal only represents the intensity of an emotion rather than its type.

The electrodes used in GSR measurements are sensitive to changes in sweat gland activity and electrical (ionic) activity. The measurements rely on the detection of changes in electrical (ionic) activity; these electrodes can send this data to the recording device. An Ag/AgCl (silver chloride) contact point connects most contemporary GSR electrodes to the skin. Ag/AgCl electrodes are employed because they are affordable, long-lasting, safe for human contact and capable of accurately transmitting the ionic activity signal. Ionic gel is applied to the electrodes to produce the same result, or it might be bundled with some electrodes to improve signal quality. In either case, the signal travels from the electrode to the wire, typically a lead, which transmits the data to the GSR equipment. Furthermore, the information is wirelessly transferred to a computer system, saved on the device for subsequent upload, or relayed to a computer via a second connection. Skin electrodes are a simple tool for measuring skin conductance. Skin conductance is collected at sample rates between 1-10 Hz and measured in micro-Siemens ( $\mu\text{S}$ ), which is the unit of measurement derived from data capture.

Research involving EDA has been reported in practically all areas of psychology, psychiatry, and psychophysiology. Beginning with fundamental studies that examine attention, information processing, and emotion to more applicable clinical studies that look at predictors and/or correlations of normal and pathological behavior, EDA measures have been used to study a wide range of subjects. The application of EDA measures addresses a wide variety of issues due to its low cost, relative ease of measurement and quantification, combined with its sensitivity to psychological states and processes. Individuals with variations in the autonomic nervous system are affected by heart rate and heart rate variability. The motor abnormalities, which are indicative of behavioral deregulation, are detected by EMG, which analyzes muscle activity. Subjects with abnormal behavioral states frequently have aberrant facial muscle movements, which are associated with problems expressing their emotions. Anxiety, agitation, or paranoia are typical during psychotic episodes and are indicated by increased muscle tension, particularly in the face. EMG is also used to identify difficulties with movement or catatonia, which might be a symptom of schizophrenia.

Many researchers have conducted studies on mental health analysis to understand the difference between psychosis and psychiatric risk [1], [3]. Loud thoughts or perceptions are a hallmark of psychosis (PSY), and they are intimately linked to Source Monitoring (SM), which is the capacity to distinguish between internal and external sources of experience [2]. Although there may be noticeable inter-individual differences in how psychotic diseases manifest, respond to therapy, and relapse, overall, these individuals receive equivalent clinical treatment. The goal of precision psychiatry is to treat each patient uniquely by classifying individuals with

a particular condition based on several clinical outcomes. Currently, it is challenging to anticipate inter-individual differences in the prognosis of psychotic diseases based solely on clinical examination. Thus, contemporary research in psychosis aims to combine clinical data with several biological parameters to create models that forecast outcomes. The most recent advancements in the treatment of psychotic disorders using precision psychiatry are reviewed here, along with the challenges of using this approach in a clinical context [3].

The abnormal behavior characteristics focuses on various nonlinear signal detection and biosensor data patterns. The GSR biofeedback method [4], is applied to a cutting-edge neurorehabilitation technique for people with mental illnesses. Treatment strategies that combine pharmacological treatment with therapies that improve functioning are evaluated for a variety of mental disorders. To diagnose mental disorders, the GSR, Skin Conductance Responses (SCR) and Skin Conductance Level (SCL), physiologic parameters are measured [4]. The significant role of GSR in the detection of emotional response, stress and anxiety is highlighted in the comparative study and the experimental work carried out [4], [8], [11], [12]. The GSR sensor data is pre-processed by being subjected independently to ensemble learning models and traditional machine learning, respectively, for comparison and performance metrics measurement [5]. However, the current era is characterized by constant change, intense social competitiveness, elevated stress levels, and a rising prevalence of mental health issues. Individuals with chronic and ongoing mental health issues may have severe mental illnesses or losses. However, to have a sustainable solution for mental health illnesses, there is a significant need for real-time data validation for precision and robust design of smart wearable device. Smart sensors have been increasingly significant in the monitoring of mental health in recent years [6]. Wearable technology data from the real-world might provide insight into mental health in day-to-day living to find if the Fitbit, a wearable device, can accurately sense it [7]. Additionally, measuring movement using optical pulse Photoplethysmography (PPG) and a 3D accelerometer could be used to estimate mental health status.

A multimodal data set [8] of human-affective states was employed, comprising peripheral physiological signals and Electroencephalogram (EEG) recordings of participants' instantaneous responses to emotionally charged video clips. Machine learning methods were applied, namely, Decision Tree (DT), Linear Regression (LR), and Long Short-Term Memory (LSTM), to model changes in Heart Rate and GSR. People consistently restrict GSR to use solely for stress detection. Another area where GSR employed is in drowsiness detection [9]. Therefore, increasing the use of GSR in sleepiness detection is the challenge of this study. Due to their never-ending workload, drivers, employees, and students all struggle with sleep deprivation. Consequently, drowsiness detection is necessary to avert unplanned mishaps. Since the recording is always done on the wrist and hand motions could affect the reading, the current GSR application for sleep deficiency detection needs improvement in data reliability. Thus, for trustworthy data or activities, an additional drowsiness detection technique is required.

A coherent study aimed at the early detection of Autism Spectrum Disorder (ASD) [10] using routinely collected developmental surveillance data from over 1.18 million children in Israel. In fact, this study demonstrates that machine-learning models—particularly gradient boosting methods such as LightGBM can effectively classify ASD risk as early as 12 months of age, achieving an Area under Curve (AUC) of 0.83 with high specificity. This work focuses specifically on early childhood ASD detection; it highlights the potential of machine learning techniques applied to structured health records for the early identification of complex neurodevelopmental conditions. This research paper highlights the application of machine-

learning models such as gradient boosting methods for neurodevelopmental disorders [10], [18]. Connectivity between electrodes increases as sweat, containing water and electrolytes, lowers the electrical resistance of the skin. Measurements are activity occurring due to a stimulus. Phasic activities can occur on top of tonic activity. Tonic activity is the constant background activity of sweat glands and their afferent innervating neurons, denoted by the word "level" at the end of terms (e.g., Skin Conductance Level). Global increases in physiological arousal reflect an increase in EDA, which is often interpreted as predominantly reflecting Sympathetic Nervous System (SNS) activity [11]. From a spider-fearing individual, bio-signals such as Electrocardiogram (ECG), Electro-dermal activity, and respiration data were collected with the help of a wearable sensor [12]. The collected data evaluated the level of anxiety through bio-signals. The effectiveness of machine learning models in classifying anxiety levels using these physiological data is demonstrated. Similarly, a system for detecting driver anxiety using multimodal bio-signals has been developed. The feasibility of using physiological signals to detect anxiety in various contexts is confirmed in this study. Using the trained machine learning models, the validation of bio signals was performed. Anxiety levels and driver distraction are key contributors to road accidents. This highlights the importance of this study in real time scenarios [12], [9].

Using multimodal biosignals and machine learning models, the driver's anxiety level is detected. By utilizing biosignals, feasibility enables the detection of the anxiety level invoked in any situation. Using physiological sensors and quantifying skin conductance, identification of distraction is achieved. Deconvolution techniques are applied to raw skin conductance signals to obtain the phasic and tonic components. Identification of normal driving versus distracted scenarios is done by training various classifiers. Heart rate and body temperature significantly transform as changes in emotions are expressed in gestures, facial expressions, voice, posture, and behavior [13]. Modern technologies and their usefulness in providing possible directions for research in emotional expressions are reviewed.

The diagnosis of depression is done using machine learning methods, including Electroencephalography (EEG) and neuroimaging data [14]. EEG, eye tracking, and GSR information have been recorded from one hundred and forty-four depression patients, achieving 79.63% accuracy with the Logistic Regression technique. The responsiveness of skin reactions varies in relation to changes in brain activity. Human sentiment analysis is conducted based on multimodal dataset development using customized physiological sensors [15]. Heart rate and GSR data from 31 volunteers are elicited using video clips [16]. Studies have reported analysis of emotions in relation to various physiological responses.

Psychosis is a mental disorder characterized by disruptions in thought processes, perceptions, and emotional responsiveness, involving symptoms like hallucinations, delusions, disorganized thinking, and social withdrawal [1], [2]. However, psychiatric risk reflects the likelihood of developing mental health issues or exhibiting abnormal behavioral and emotional states without losing touch with reality. The potential benefits of this research include the development of non-invasive and cost-effective tools for early psychiatric risk detection, which could facilitate timely intervention and improve treatment outcomes [6], [21], [22]. The proposed framework involves collecting sensor data from participants during various tasks or stimuli designed to elicit physiological responses related to behavioral deregulation in adolescents. The integration of GSR, pulse, and EMG sensors with the Arduino UNO and subsequent optimization of the power supply resulted in stable and reliable operation of the sensors. The improved data quality confirms the success of the corrective measures.

Literature review [17]-[18] shows bio signals that reflect a person's health directly help to detect physiological arousal, acute mental stress, the effect of meditation, emotional response, and autism spectrum disorder among individuals invoked in multiple situations [19], [20]. In total, 48 papers were reviewed [21], where the findings indicate 60% of studies related to stress samples, followed by depression at 31% and anxiety at 9% of research studies. Disturbances in emotional and cognitive control, as well as behavioral abnormalities, are closely associated with psychiatric problems. However, for the early identification of mental health issues, there are few standard clinical instruments available [22].

There is a crucial need to identify the biomarkers for quick and real-time monitoring for the prevention and prognosis of mental illness. This review discusses mental illnesses that have high rates of sickness, disability, and death before outlining the pathophysiology in a way that suggests biomarkers. The significant advancements made before psychiatric treatment may move from clinics to people's everyday lives [23]. The optimization technique based on biological inspiration, the jellyfish search optimization technique, is introduced. Biosensors such as heart rate, GSR, and skin temperature sensors are used in collecting physiological and behavioral data, which are analyzed by SVM, decision trees, and neural networks for monitoring mental health [5], [16], [20]. A survey of technologies, devices, and methods in the mental health monitoring field was carried out, where the original experimental data were not reported [24]. Important investigations have been conducted on the mental and physical disability of individuals affected by Endosulfan spray. The Endosulfan-affected adolescent victims and caregivers are suffering in their lives due to neural disorders, which requires support to lead a better life. In addition, there is a requirement for the collection and analysis of bio signals using biosensors for real-time monitoring [25]. In summary, studies conducted on abnormal behaviors identify a lack of cost-effective and indigenous systems for bio signal acquisition and processing. There is a crucial need to study multiple modalities of the data sets, sustainable accuracy and precision models, and a robust experimental setup. The analysis of transform domain features is observed using advanced nonlinear non-stationary signal processing. Additionally, for the acquisition and analysis of the bio signal, the model must select and train the conditions for psychiatric risk detection.

The proposed study addresses the following objectives to overcome the limitations of bio sensing systems for psychiatric risk detection:

- Design a multimodal framework with the integration of biosensors such as pulse, EMG, and GSR.
- Extract relevant features from the dataset to capture neuromuscular changes linked to behavioral disturbances, stress, and arousal in subjects.
- Evaluate machine learning models in the correct classification of abnormal behavioral and psychiatric risk states from the physiological signals.
- Establish timely support for caregivers and healthcare providers in the early identification of behavioral and emotional deregulation.

This paper is further organized into the following parts: Section 2 illustrates the dataset extracted for this study, followed by the methodology for multi-class psychiatric risk detection. Sections 3 and 4 explain the results and conclusions, respectively.

## 2. Materials and Methodology

The main objective of this work is to develop a machine learning framework for the classification of individual subjects into low-risk and high-risk categories. This section describes the method designed for collecting physiological signals and the analysis methodology.

### 2.1 Data Acquisition Through Sensor Module and Testing

The psychiatric risk detection takes a crucial leap forward during system implementation to tackle real-world challenges. The system for acquisition, detection, and analysis of psychological risks is represented in Figure 1, using a multifaceted strategy. In this study, the conception of software modules, such as data gathering modules, machine learning models, and signal processing algorithms, takes center stage in software development. These precisely coded parts are subjected to a rigorous testing process that guarantees perfect alignment with the objectives of the research.

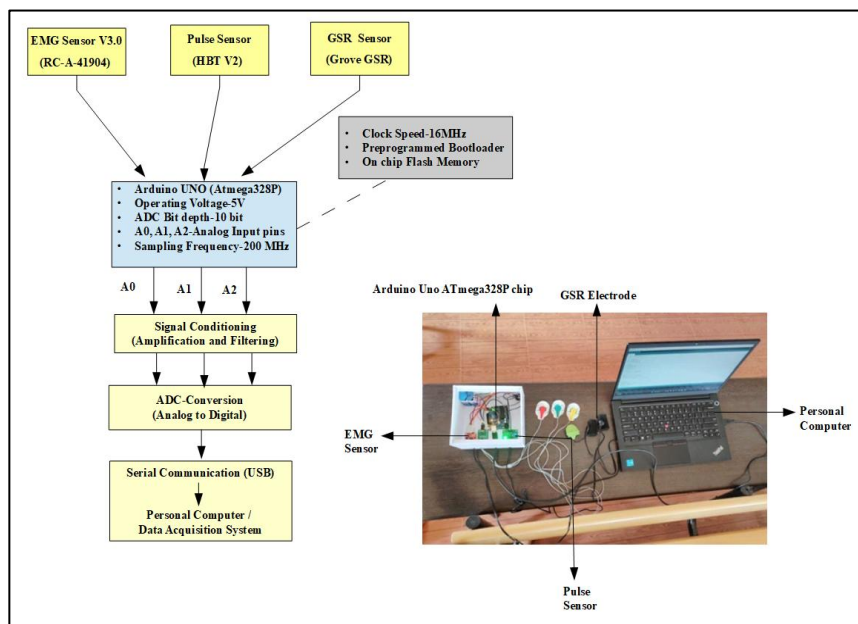


**Figure 1.** Data Acquisition Process Using Physiological Sensors

Hardware integration powers the system in parallel. The system is seamlessly integrated with sensors to record physiological signals such as pulse, EMG, and GSR. Deploying the system in clinical settings involves careful preparation for both installation and training. This effective theory-to-practice translation offers hope for early psychiatric risk detection and care, which could enhance patient outcomes and quality of life.

The system represented in Figure 1 utilizes an Arduino UNO microcontroller (ATmega328P) due to ease of programming and versatility. The pre-programmed bootloader on the Arduino microcontroller simplifies the process of uploading programs to on-chip flash memory. GSR (Grove-GSR), pulse (HBT V2 heart rate sensor), and EMG Muscle Sensor V3.0 are used to acquire electrodermal activity, pulse, and small electrical signals generated by the change in muscle activity. The sensor analog outputs are sampled with a delay of 5 ms between the readings. The resulting sampling frequency is 200 Hz. Using a single Arduino UNO to acquire the EMG, GSR, and pulse signals with the help of analog input channels, cross-modal

synchronization is achieved. All the signals are sampled in the same acquisition loop with the 16 MHz microcontroller clock, ensuring minimal temporal delay among the modalities and ensuring time-synchronized physiological readings. This integration of various modules is used to create a database. Important investigations have been conducted on subjects regarding the long-term effects of Endosulfan spray disability [33] [34].

In this study, bio-signal response data were acquired from mentally challenged subjects belonging to the Sanidhya Skill Training Centre for Endosulfan victims in Ujire, Karnataka State, India, which was established under the collaboration of the Dakshina Kannada District Health and Family Welfare Department (<https://www.saanidhya.org/>).

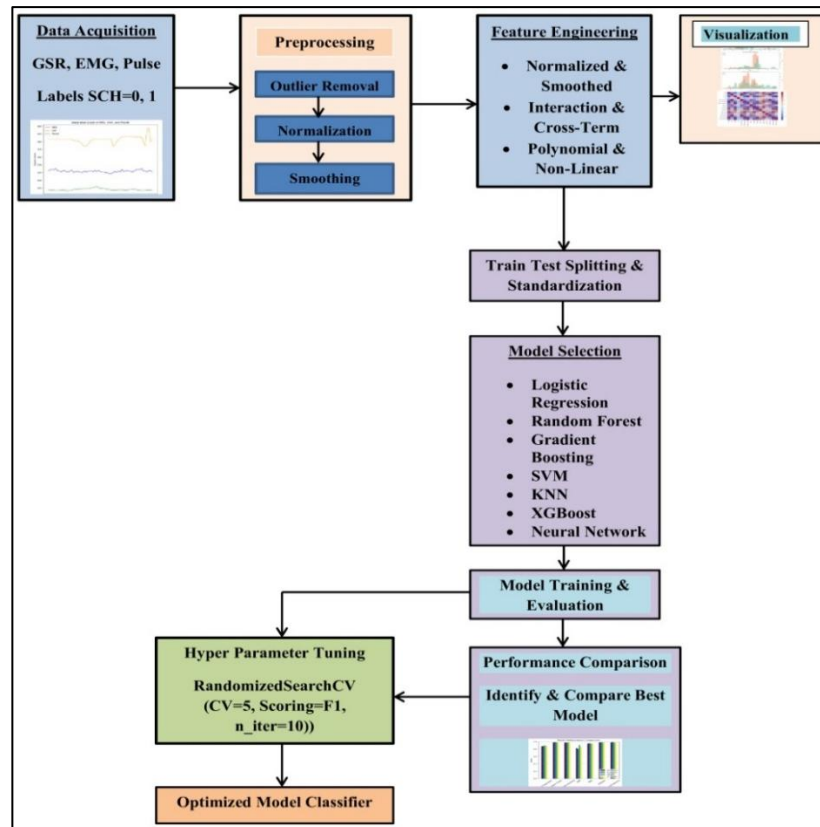


**Figure 2.** Taxonomy for Detection of Physiological Response to Identify the Psychiatric Risk and Abnormal Behavioral States

A total of 66 subjects aged  $13 \pm 2$  years were trained with ethical approval from the institution's expert team to create a sustainable database. The subjects at this institute, who are mentally challenged and exhibit symptoms of abnormal behavioral states, were supportive of this study. Informed consent was acquired from all the participants prior to data collection. Data validation was conducted by a medical expert from Pragathi Specialty Hospital, Puttur, Karnataka State, India. The multimodal bio signals such as EMG, GSR, and pulse were acquired and tested under medical supervision.

In addition, during the acquisition of these physiological signals, careful preventive measures were taken. Figure 2 represents the flow diagram to detect the physiological response after the data acquisition shown in Figure 1. The dataset includes ECG, GSR, and pulse data along with Sensor Captured Health (SCH)=0/1 as attributes. The dataset was obtained from the training center where the subjects exhibited abnormal behavioral states, and the validation of

the dataset was performed at the hospital, excluding the standardized psychiatric screening scores. A direct comparison with respect to the psychiatric screening tool was not performed.

## 2.2 Filtering and Descriptive Statistics

In this paper, the acquired bio signals, which form the dataset, undergo further processing using the Inter Quartile Method (IQR), as shown in Equations (1)-(5), to remove outliers. The filtered dataset is divided into two groups, namely the Higher Risk Group (SCH=1) and the Lower Risk Group (SCH=0), followed by the computation of descriptive statistics. The descriptive statistics include counting the number of valid observations in each group, mean (average value for each metric), standard deviation (amount of spread or variability of the data), minimum and maximum (smallest and largest values recorded in each group), and quartiles (data divided into four equal parts).

The physiological signal is represented as  $X$  where,

$$X \in \{GSR, EMG, pulse\} \quad (1)$$

The first and third quartile is represented as:

$$Q1 = 25^{\text{th}} \text{ percentile of } X \text{ and } Q3 = 75^{\text{th}} \text{ percentile of } X \quad (2)$$

The Interquartile range is shown as:  $IQR = Q3 - Q1$  (3)

The upper and lower bound is represented as: (4)

$$\begin{aligned} \text{Lower Bound} &= Q1 - 1.5 * IQR \\ \text{Upper Bound} &= Q3 + 1.5 * IQR \end{aligned}$$

A data point  $x_i$  is considered as outlier if:

$$\begin{aligned} x_i &< Q_1 - 1.5 * IQR \quad \text{or} \\ x_i &> Q_3 + 1.5 * IQR \end{aligned} \quad (5)$$

A sample  $i$  is removed if any of the physiological feature falls outside the range as specified in Equation (5) and is represented in Equation (6):

The statistical threshold value of 1.5 in Equation (6) is the widely accepted value for the detection of moderate outliers and it provides balance between the removal of the abnormal spikes and retaining the physiological variability.

$$\begin{aligned} \exists X_j \in X \text{ such that } x_i^{(X_j)} &< Q_1^{(X_j)} - 1.5 IQR^{(X_j)} \text{ or} \\ x_i^{(X_j)} &> Q_3^{(X_j)} + 1.5 IQR^{(X_j)} \end{aligned} \quad (6)$$

The physiological signals can contain abrupt variations due to the presence of sensor noise or artifacts. The non-parametric methods are more suitable than mean deviation-based techniques. The IQR is mainly based on 50% of the physiological data ( $Q1-Q3$ ), with no influence from extreme values, making it highly suitable for bio-signal processing. The removal of extreme outliers before normalization and feature engineering prevents distortion in the model.

The original dataset consisted of a total of 793 samples in the class SCH=0 and 750 samples in the class SCH=1, for a total of 1543 samples. When the IQR-based outlier removal is performed, as shown in Equations (2)-(6) across the three physiological signals presented in Equation (1), 308 samples, nearly 38.84%, were removed from the class SCH=0, and 113 samples (15.07%) were removed from the class SCH=1. The final filtered dataset consisted of a total of 1122 samples: 485 samples in the SCH=0 class and 637 samples in the SCH=1 class. Although a larger portion of samples was removed from the SCH=0 class (38.84%) compared to the SCH=1 class (15.07%), this indicates a greater presence of extreme physiological values in the lower-risk group. The difference in the values represents inherent distributional variability rather than selective exclusion, as the IQR is applied uniformly to both classes and the IQR threshold is globally calculated across the entire dataset. A total of 1122 samples are present in the final filtered dataset, which includes 485 samples in the SCH=0 class and 637 samples in the SCH=1 class; this dataset is used for feature engineering and model deployment.

The key statistics, such as mean, standard deviation, and percentiles, are represented in Figure 3 for the GSR, EMG, and pulse across the healthy and psychiatric risk groups. However, there are more participants in the psychiatric risk group (637) compared to the non-psychiatric risk group (485), which leads to an increase in statistical power and makes it easier to identify differences. Moreover, this study finds that the bio-signal pulse is modestly elevated, indicating potential heightened arousal. In contrast, the biosensor signals for GSR and EMG values are generally greater in the psychiatric risk group, showing increased skin conductance and muscular activity.



**Figure 3.** Representation of Descriptive Statistics in a Heatmap After Filtering of Biosensor Signals

The psychiatric risk group's smaller standard deviation across all the measurements (GSR: 46.71 vs. 60.31, EMG: 40.01 vs. 49.53, Pulse: 7.79 vs. 10.81) is a noteworthy trend that suggests less variability in physiological responses. This might be the result of less adaptive but more consistent physiological activity brought on by a dampened autonomic nervous system. Furthermore, the maximum values for GSR and EMG are consistent across the groups, suggesting no notable outliers at the higher end, and the minimum values are higher in psychiatric risk, suggesting fewer extremely low responses. In fact, analyzing the percentiles, psychiatric risk is consistently associated with higher median (50%) levels, which supports the idea that physiological activity is elevated. Additionally, the psychiatric risk group's narrower IQR indicates a smaller variance in their physiological reactions. The psychiatric risk group's higher mean, meanwhile, along with the smaller standard deviation, suggests that the

physiological responses of the subjects are persistently increased and less variable, which may be a crucial biomarker for the identification of psychiatric risks. This pattern may indicate an active stress response system or dysregulated autonomic nervous system activity. Knowing these physiological indicators can improve early detection techniques and enable data-driven, unbiased evaluations of psychiatric risk. These results demonstrate the possibility of using physiological monitoring in clinical diagnostics to increase the precision of differentiating between healthy controls and those suffering from psychiatric risk. The statistical tests performed multiple times increase the probability of obtaining at least one false positive result; i.e., the Type I error rate increases. This probability is referred to as the Family-Wise Error Rate (FWER). In order to control this error rate, the Bonferroni correction, as shown in Equation (7), is applied. The corrected value of the significance level is:

$$\alpha_{corrected} = \frac{\alpha}{m} \quad (7)$$

where  $\alpha$  is original significance level (0.05) and  $m$  represents the number of hypothesis test here it is 3 as statistical test is performed on 3 physiological features.

$$\alpha_{corrected} = \frac{0.05}{3} = 0.0167$$

The Bonferroni-adjusted p-value is:

$p_{corrected} = m * p_{original}$  where  $p_{original}$  is the independent t test obtained p-value

**Table 1.** Independent t-test with the Bonferroni Correction

Features	t-Statistic	Original p-value	Bonferroni Corrected p-value	Significant (after correction)
GSR	-12.885	$6.07 \times 10^{-35}$	$1.82 \times 10^{-34}$	True
EMG	-3.818	$1.44 \times 10^{-4}$	$4.31 \times 10^{-4}$	True
PULSE	-4.849	$1.48 \times 10^{-6}$	$4.44 \times 10^{-6}$	True

In Table 1, since all the corrected p-values are lower than the threshold ( $\alpha_{corrected} = 0.0167$ ), which indicates the statistical significance between the two groups.

### 2.3 Feature Extraction

The activation of the autonomous nervous system associated with emotional and physiological responses is called physiological arousal. It reflects the sympathetic nervous system activation quantified by physiological signals.

Consider for each sample ( $i$ ), the biosensor signals GSR, EMG, and pulse, which are typically represented in Equation (8) as:

$$x_i = [GSR_i, EMG_i, Pulse_i] \quad (8)$$

The physiological arousal is defined using Equation (9) as:

$$A_i = f([GSR_i, EMG_i, Pulse_i]) \quad (9)$$

where,  $f(.)$  represents the relationship that is being learnt by the classification models. Higher value of this function indicates increased physiological arousal due to increased autonomic nervous system activation.

In this study, a total of 15 features were extracted from the raw physiological signals such as GSR, EMG, and pulse. Extracted biosensor variables include raw features, normalized features, squared features, moving averages, and cross-product features. The normalization process scales the data to a standard range (commonly  $[0, 1]$ ) or a mean of 0 with a standard deviation of 1).

The min-max normalization is represented using the Equation (10)-(11):

$$X_i^{norm} = \frac{X_i - X_{min}}{X_{max} - X_{min}} \quad (10)$$

where,  $X_i$  denotes feature X value for sample i,  $X_{min}$  and  $X_{max}$  are minimum and maximum value of feature X in the dataset.

The z-score normalization represented by:

$$X_i^{std} = \frac{X_i - \mu_X}{\sigma_X} \quad (11)$$

where, the variables  $\mu_X$ ,  $\sigma_X$  represents the mean and standard deviation of feature X, respectively for the physiological signal.

The squared signals are used to emphasize the signal energy, which is useful in GSR and EMG signals. The transformation in Equation (12) highlights the higher values in the intensity levels.

$$X_i^{(2)} = (X_i)^2 \quad (12)$$

The Moving Average (MA) in Equation (13) that polishes the short-term fluctuations and the longer-term trends.

$$x_{MA}(t) = \frac{1}{w} \sum_{k=0}^{w-1} x_{i-k} \quad (13)$$

Here, (w) is the window size (the value taken as 3) and (i) is the ordered current sample index.

The cross features, or interaction features, represented in Equations (14) and (15), are extracted by combining two signals to capture the correlation between the signals.

$$GSR\_EMG = x_{GSR} * x_{EMG} \quad (14)$$

$$EMG\_PULSE = x_{EMG} * x_{PULSE} \quad (15)$$

These features uncover the physiological patterns between the two combined signals.

## 2.4 Classification Using Machine Learning

In this stage, preprocessed biosensor data is converted to the transform domain for significant feature extraction, and a suitable machine-learning algorithm is implemented to detect psychiatric risk or physiological arousal occurrence. In this paper, for classification, conventional machine-learning methods such as Logistic Regression, Random Forests, Gradient Boosting, Support Vector Machines (SVM), K-Nearest Neighbors (KNN), XGBoost, and Neural Networks are applied. Subsequently, comprehensive assessment methods are used to validate the accuracy, providing insightful information for correctly identifying psychiatric

risks. However, the systematic analysis of the nonlinear and non-stationary biosensor signals advances the development of objective detection against subjective observation using efficient non-invasive techniques. The data classification of machine-learning classifiers is briefly explained as follows: The strength of supervised learning is exemplified by the KNN approach, which is applied to regression and classification problems. Considering feature similarity, KNN evaluates a new data point's proximity to an existing one in the training set to predict the class or continuous value. This method emphasizes the significance of neighbor selection based on the parameter  $K$ . In addition, the KNN classifier illustrates that the majority class among the nearest neighbors determines the categorization of a new data point and is robust for multi-class classification of large volumes of data.

Gradient Boosting is an ensemble learning technique that builds models in a sequential fashion, with each new model correcting past errors. The gradient descent method is applied to optimize performance, in which the decision trees act as weak learners. Additionally, for structured data, Gradient Boosting performs significantly, although computational cost is a constraint.

Data categorization measures are the primary application of the traditional machine-learning classifier SVM. To determine which class a new data point belongs to, the basic idea requires separating the available data points into multiple classes. Based on the class labels assigned to the data points, SVM treats them as vectors in a multidimensional space and searches for a hyperplane that splits the points into useful segments. The variables have two category alternatives in binary classification tasks, namely the presence or absence of psychiatric risk. The binary classifier logistic regression is a popular statistical technique for transforming the linear combination of input data into nonlinear probabilities between 0 and 1 using a logistic function.

XGBoost is an enhanced version of Gradient Boosting that is a faster and more efficient algorithm, which supports parallel processing, regularization, and advanced tree pruning. It also minimizes overfitting while improving accuracy, making it widely useful in competitive machine learning to achieve high performance, especially in tabular datasets.

A popular ensemble learning approach for classification and regression problems is Random Forest. To arrive at a final prediction, Random Forest builds several decision trees using various subsets of the training data characteristics, resulting in combined trees. The name "Random Forest" stems from the randomness introduced during the tree-building process, which includes the random selection of data samples and features for each tree. This randomness helps to prevent the overfitting problem and results in a robust and accurate model.

An example of a feedforward artificial neural network that uses backpropagation for learning is the Multi-Layer Perceptron (MLP) classifier. It consists of input, hidden, and output layers with activation functions like Rectified Linear Unit (ReLU) or sigmoid. MLP is powerful for non-linear data; however, it requires a large volume of data and tuning compared to tree-based models.

### 3. Results and Discussion

The first stage in developing a machine-learning model involves assembling the required real-time dataset manually. In a variety of settings, pulse, EMG, and GSR biosensors gather significant physiological parameters (time-domain), which undergo pre-processing to

turn the raw data into a clean dataset. In order to make exploration and trend analysis easier, this process demands eliminating duplicates, dealing with missing values, and normalizing obtained results. Considering the best features extracted, an appropriate classification method is chosen to produce sustainable results. The trained model undergoes testing to assess its accuracy in predicting unseen data.

### 3.1 Time Domain Representation of Biosensor Signal

The collective time-domain graph of the skin resistance obtained using the GSR, muscle contraction from EMG, and pulse interpretation of an individual is represented in Figure 4. The orange line in Figure 4 depicts muscle contraction; the blue line reflects skin resistance, whereas the green line reflects pulse sensor recordings.

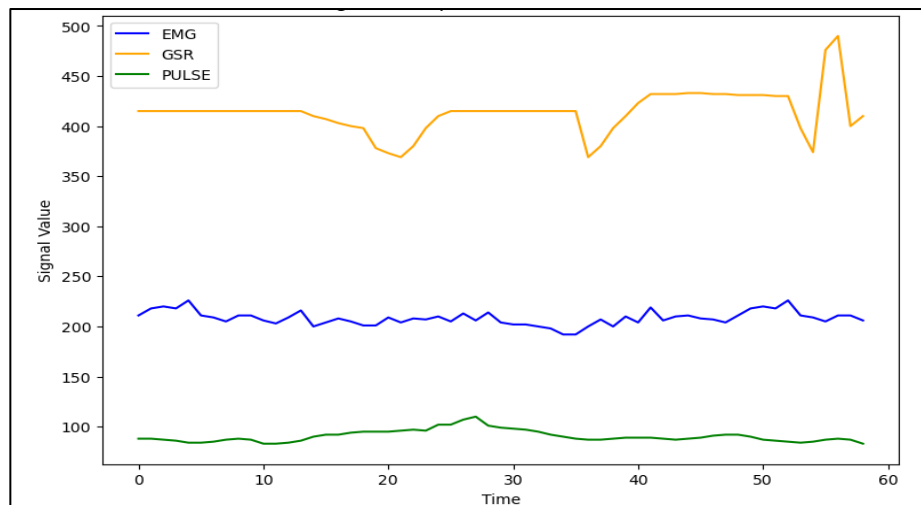


**Figure 4.** Time Domain Representation of GSR, EMG and Pulse Biosensor Signals

Figure 5-7 represents the typical plot of the percentage of physiological arousal in a subject, where the data is collected via the integrated sensor module. The dataset is acquired as per Figure 1. The obtained signal is a combined dataset. In addition, the outliers are eliminated by applying the IQR. The filtered data is divided into two groups, and descriptive statistics, namely count, mean, standard deviation, minimum and maximum, and quartiles are calculated.

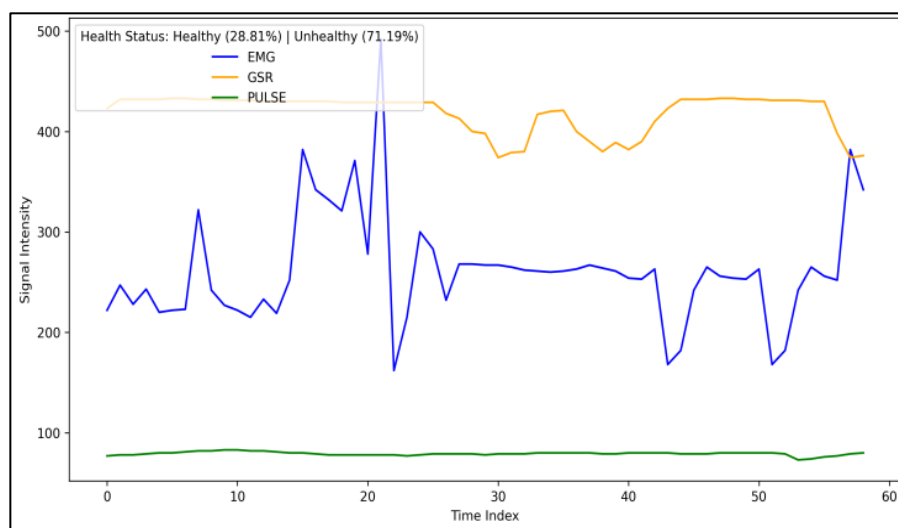


**Figure 5.** Percentage of Occurrence 71.19% of Psychiatric Risk /Physiological Arousal in a Psychiatric Subject

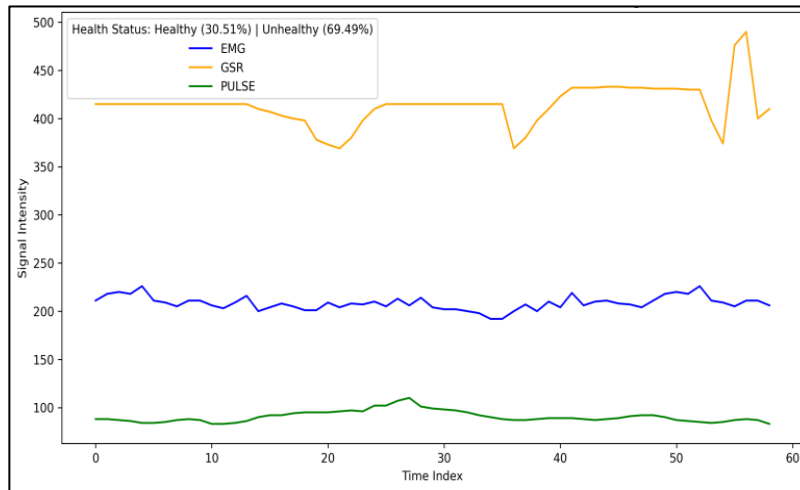


**Figure 6.** Percentage of Occurrence 69.49 % of Psychiatric Risk /Physiological Arousal in a Psychiatric Subject

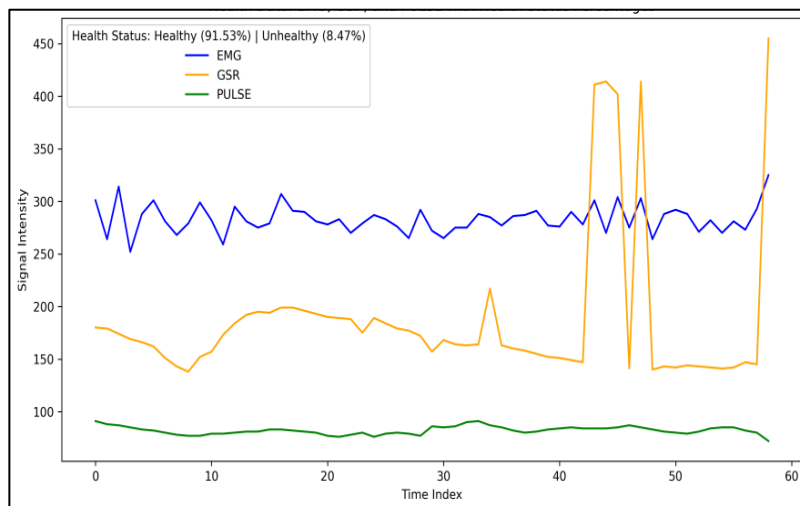


**Figure 7.** Percentage of Occurrence 8.47 % of Psychiatric risk /Physiological Arousal in a Healthy Subject

Figures. 8-10 represent the histogram and kernel density estimation (KDE) plot of GSR signals. The subject with no psychiatric risk is represented in green (SCH=0), while the subject with psychiatric risk is represented in orange (SCH=1). Each plot contains histogram and KDE curves for data visualization. In Figure 8, the values of the GSR signal range from 200 to 500. The Y-axis shows the frequency of occurrence of the multiple GSR values. The psychiatric risk group has a higher peak around the 400 GSR value, whereas the non-psychiatric risk group has a broader distribution. In Figure 9, the EMG values on the X-axis range from 100 to 350. The psychiatric risk group has a higher peak around 200 for EMG, whereas the non-psychiatric risk group has a more spread-out distribution. Figure 10 represents the pulse values on the X-axis ranging from 60 to 100 beats per minute (BPM). The psychiatric risk group has a peak around 80 BPM, while the non-psychiatric risk group has a wider distribution. The smooth estimate of the probability distribution for each group is obtained by the KDE plot.

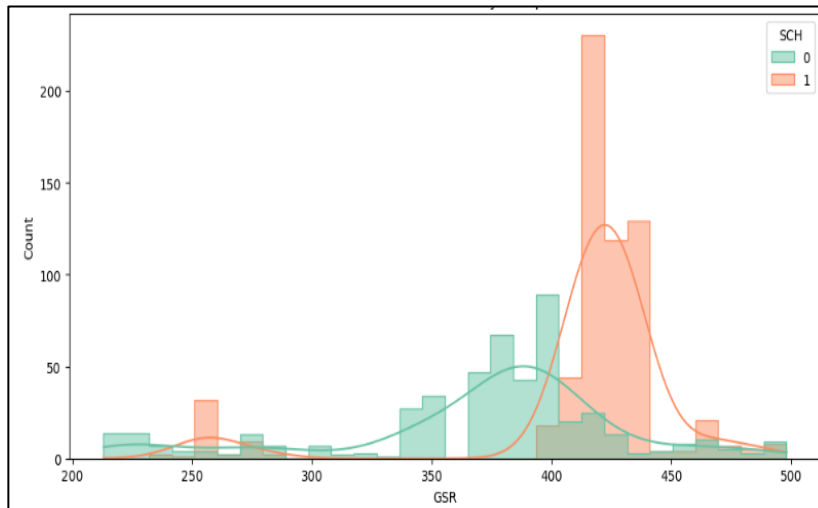


**Figure 8.** The Histogram and Kernel Density Estimation (KDE) Plot Illustrate Distribution of GSR Signals

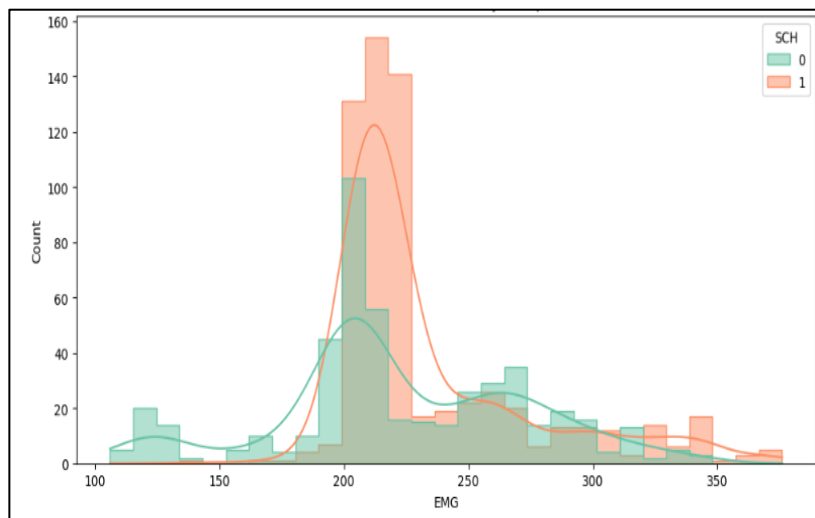


**Figure 9.** The Histogram and Kernel Density Estimation (KDE) Plot Illustrate Distribution of EMG Signals

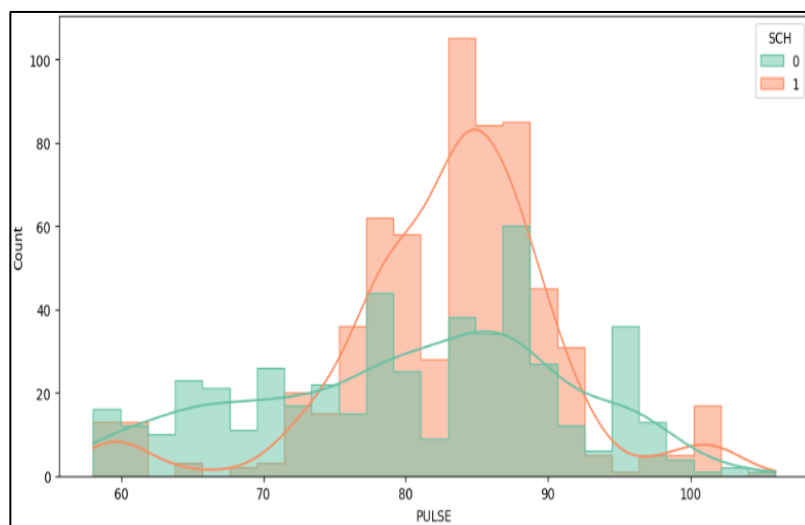


**Figure 10.** The Histogram and Kernel Density Estimation (KDE) Plot Illustrate Distribution of Pulse Signals

### 3.2 Representation of Features and Classification

The extracted features, such as normalized values (GSR, EMG, and pulse), moving average, and feature combinations, are used to capture interactions between signals and polynomial features and to visualize non-linearity. In total, 15 features are extracted, and their correlation is shown in Figure 11. This provides a comprehensive overview of the linear relationships among the three physiological signals and their computed derivatives used for psychiatric risk detection. Combined with pulse data, the EMG signal exhibits a very high positive correlation with both EMG\_squared (0.99) and EMG\_PULSE (0.81), demonstrating great internal consistency and relevance. As predicted by mathematical modifications, pulse also shows a nearly perfect association with PULSE\_normalized and PULSE\_squared (both 1.00). The high correlation (up to 0.99) between GSR-related features like GSR, GSR\_normalized, and GSR\_squared and combined features like GSR\_PULSE (0.79) and GSR\_EMG (0.74) indicates that GSR data plays a substantial role in combined feature sets. Their usefulness in temporal smoothing is supported by the reasonable correlations that moving averages (such as EMG\_MA and PULSE\_MA) exhibit with their original signals (0.85–0.94). Following feature extraction, a supervised machine learning pipeline is implemented for classification, which includes multiple models to predict the target variable SCH.

The process involves data preprocessing, model training, evaluation, and hyperparameter tuning for performance optimization. The dataset is divided into 70% for training and 30% for testing, using stratified random sampling to preserve class distribution. Each sample is taken as an individual observation; no subject-wise splitting is performed, and no grouping or subject identifier is used. Standardization (StandardScaler) is applied to logistic regression and neural models to normalize feature distributions. The scaler is fitted only on the training data to prevent data leakage, and the learned parameters are used to transform both the training and testing sets. After splitting, standardization using StandardScaler is applied.

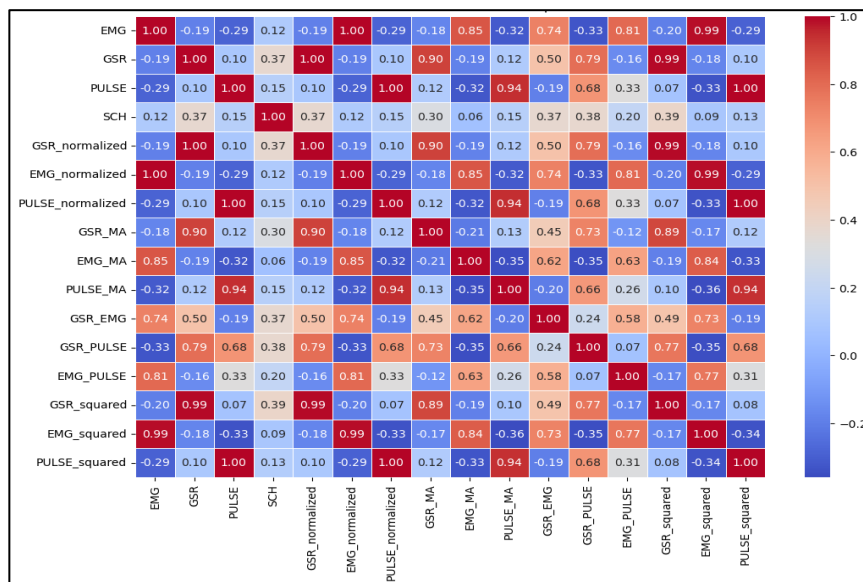


Figure 11. Feature Correlation Heatmap for Psychiatric Risk Detection

Seven classification models were implemented, and the results of the classification are shown in Table 2, which includes Logistic Regression, Random Forest, Gradient Boosting, SVM, KNN, XGBoost, and Neural Network. Each model was trained on the dataset and evaluated using multiple metrics. To improve model performance, RandomizedSearchCV was

applied to optimize key hyperparameters. Using five-fold cross-validation, hyperparameter tuning was conducted through RandomizedSearchCV, optimizing the F1 score. Hyperparameter tuning improved model performance, with optimal parameters found for Logistic Regression ( $C=100$ ), Neural Network ((100,100) hidden layers, ReLU activation), and Random Forest (200 trees, max depth 10).

**Table 2.** Summary of Classification for Healthy and Unhealthy Individuals Using Machine-Learning Models

Algorithm	Precision	Recall	F1 Score	Accuracy (%)	Confusion Matrix
Logistic Regression	0.8854	0.8901	0.8877	87.24	$\begin{bmatrix} 124 & 22 \\ 21 & 170 \end{bmatrix}$
Random Forest	0.9842	0.9791	0.9816	97.92	$\begin{bmatrix} 143 & 3 \\ 4 & 187 \end{bmatrix}$
Gradient Boosting	0.9740	0.9791	0.9765	97.33	$\begin{bmatrix} 141 & 5 \\ 4 & 187 \end{bmatrix}$
SVM	0.8047	0.9058	0.8522	82.20	$\begin{bmatrix} 104 & 42 \\ 18 & 173 \end{bmatrix}$
K-Nearest Neighbors	0.9574	0.9424	0.9499	94.36	$\begin{bmatrix} 138 & 8 \\ 11 & 180 \end{bmatrix}$
XGBoost	0.9842	0.9791	0.9816	97.92	$\begin{bmatrix} 143 & 3 \\ 4 & 187 \end{bmatrix}$
Neural Network	0.9894	0.9738	0.9815	97.92	$\begin{bmatrix} 144 & 2 \\ 5 & 186 \end{bmatrix}$

To identify the most influential features, Random Forest (RF) and XGBoost models were trained. However, Random Forest is a tree-based ensemble learning method that computes feature importance based on impurity reduction (e.g., Gini importance). On the other hand, XGBoost is a gradient boosting technique with performance and speed optimization. After the IQR-based outlier removal, the dataset contained 1,122 samples. For the machine learning process, 70% of the dataset was used for training and 30% was used for testing using a stratified split. Thus, 337 samples (30% of the data) were used for testing, and the confusion matrix represents the test dataset values.

Table 2 shows that SVM precision is low (0.8047) and recall is high (0.9058) as the model prioritized the SCH=1 class, increasing the true positive rate while also increasing false positives, which reduced precision. With an accuracy of 97.92%, Random Forest, XGBoost, and Neural Network are the most reliable models for identifying psychiatric risk in an individual. Because of their high precision and recall, these models reduce false positives, which misdiagnose healthy individuals, as well as false negatives, which fail to detect real cases of psychiatric risk. With an accuracy of 87.24%, logistic regression is easier to understand and could be helpful in clinical settings where transparency is necessary. KNN (94.36% accuracy) is useful but less scalable for large datasets. Tree-based models (Random Forest, XGBoost) are preferred for psychiatric risk prediction due to their high accuracy and ability to capture complex feature interactions. Although they work well, neural networks may require more computational resources and larger datasets. These models are used to enhance early psychiatric risk identification, resulting in prompt intervention and improved patient outcomes. The feature importance scores from the Random Forest model were extracted and visualized using a bar plot represented in Figure 12, ranking the top 15 most significant features.

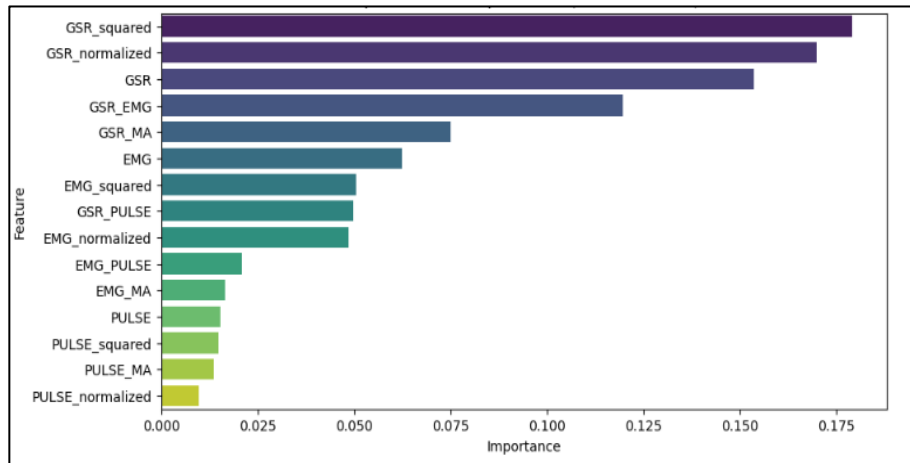


Figure 12. Ranking of 15 Features Identified by Random Forest Model

Additionally, SHAP (SHapley Additive Explanations) values are calculated using XGBoost to interpret the contribution of each feature to predictions. The SHAP summary plot in Figure 13 provides a global explanation of feature impact. To improve predictive accuracy, an ensemble model is built using a blending technique with the following models: Random Forest (RF), XGBoost (XGB), and Multi-Layer Perceptron (MLP), which is a feedforward neural network trained on the standardized feature set. Each model generates probability predictions (predict\_proba) for the positive class (SCH = 1).

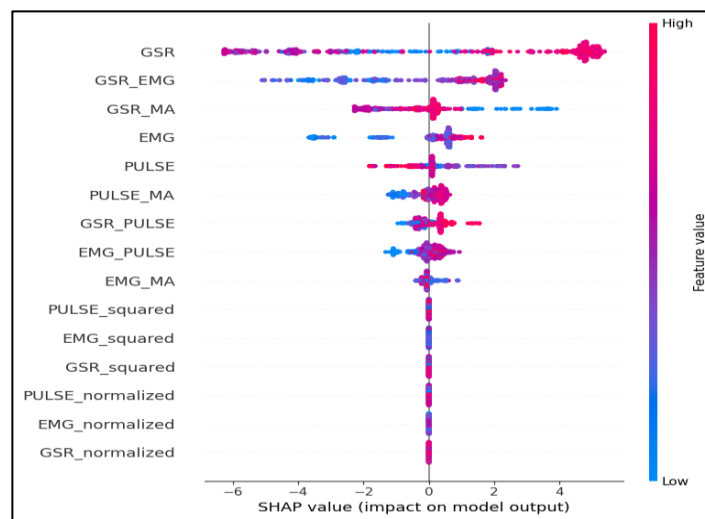


Figure 13. SHAP Summary Plot for XGBoost Model, Illustrating the Impact of Each Feature on Predictions

A weighted combination of predictions then calculated using Equation (16):

$$\text{final\_preds} = (0.4 \times \text{RF\_preds}) + (0.4 \times \text{XGB\_preds}) + (0.2 \times \text{MLP\_preds}) \quad (16)$$

Where RF and XGB are given higher weightage (40%), MLP contributes 20% due to its sensitivity to scaling and data complexity. The final predictions are converted into binary class labels using a threshold of 0.5. The performance of the ensemble model is assessed using accuracy as in Equation (17).

$$\text{Accuracy} = \text{Total Predictions} / \text{Correct Predictions} \quad (17)$$

The final ensemble accuracy obtained, as stated in Equation (17), is 98.32%, and the effectiveness of the ensemble approach is validated. In order to discern differences between individuals with psychiatric risk symptoms (SCH = 1) and those without (SCH = 0), the angle of prediction is calculated and represented as shown in Table 3 and Figures 14-15. The cosine similarity formula gives the directional change in the signal with respect to time and is used to compute the angles between successive rows of signal data. Several machine-learning techniques are examined in order to improve detection accuracy and categorize the SCH state. Angle prediction analysis offers a potential way to comprehend the physiological variations. Let the two physiological signals be defined in vector form in Equation (18) as:

$$\begin{aligned} v_{i-1} &= [EMG_{i-1}, GSR_{i-1}, Pulse_{i-1}] \\ v_i &= [EMG_i, GSR_i, Pulse_i] \end{aligned} \quad (18)$$

Using the dot product the angle  $\theta_i$  between the two vectors is computed and is shown in Equation (19)-(20):

$$\cos(\theta_i) = \frac{v_{i-1} \cdot v_i}{\|v_{i-1}\| \|v_i\|} \quad (19)$$

Where  $v_{i-1} \cdot v_i$  represents the dot product and  $\|v_i\|$  is the Euclidean norm.

The angle  $\theta_i$  is obtained by:

$$\theta_i = \cos^{-1} \left( \frac{v_{i-1} \cdot v_i}{\|v_{i-1}\| \|v_i\|} \right) \quad (20)$$

This measures the directional changes in the physiological multidimensional state space.

**Table 3.** Angle Predictions Derived from Physiological Signals

SCH	Mean	Median	Std	Min	Max	Count
0	3.9047	1.4079	6.7814	0.0000	49.8758	2671
1	2.6597	0.8501	5.0824	0.0447	45.8075	2829

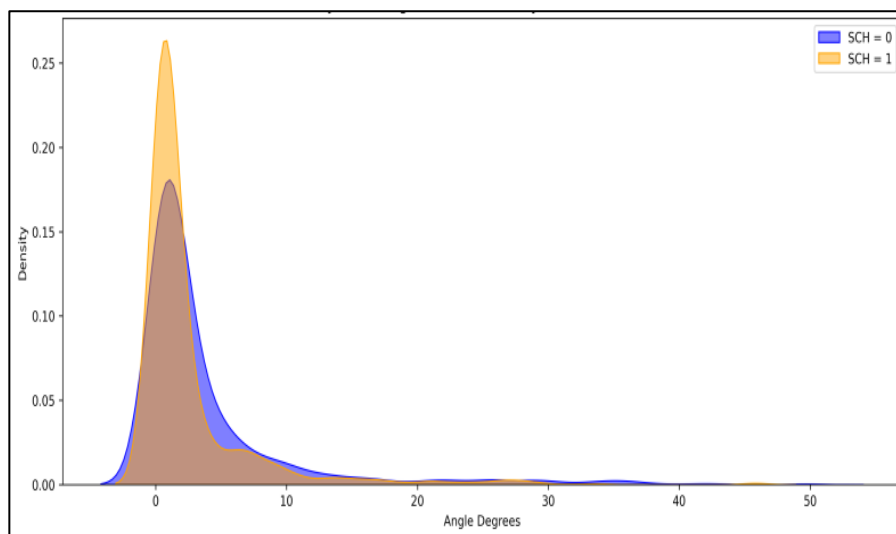


**Figure 14.** The Density Plot of Angle Prediction for Psychiatric Risk Detection

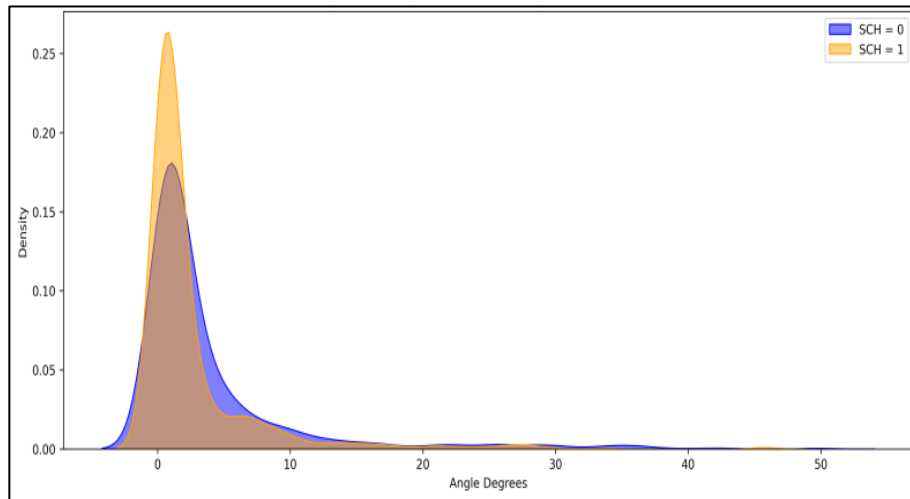


**Figure 15.** The Histogram of Angle prediction for Psychiatric Risk Detection

Based on the analysis of single-subject data, the physiological signal features are extracted, such as mean, median, variance, and standard deviation. The health state of each individual participant correlates with the retrieved features. Figure 16 represents the correlation matrix for features obtained, such as mean, median, variance, standard deviation, and health status. The heatmap identifies the correlation of the physiological features. If GSR\_StdDev (skin conductance variation) has a high correlation with PULSE\_StdDev (heart rate variability), it suggests that stress levels impact heart rate, a common sign in psychiatric risk episodes. In psychiatric risk patients, GSR may show excessive fluctuations due to abnormal autonomic nervous system activity. EMG may show reduced muscle activity due to catatonia (rigidity or lack of movement). Pulse variability may increase due to stress and panic episodes. If the heatmap shows unusual correlations, such as an unexpected negative or near-zero correlation between GSR and Pulse, it may indicate dysregulated autonomic responses, which are common in psychiatric risk.

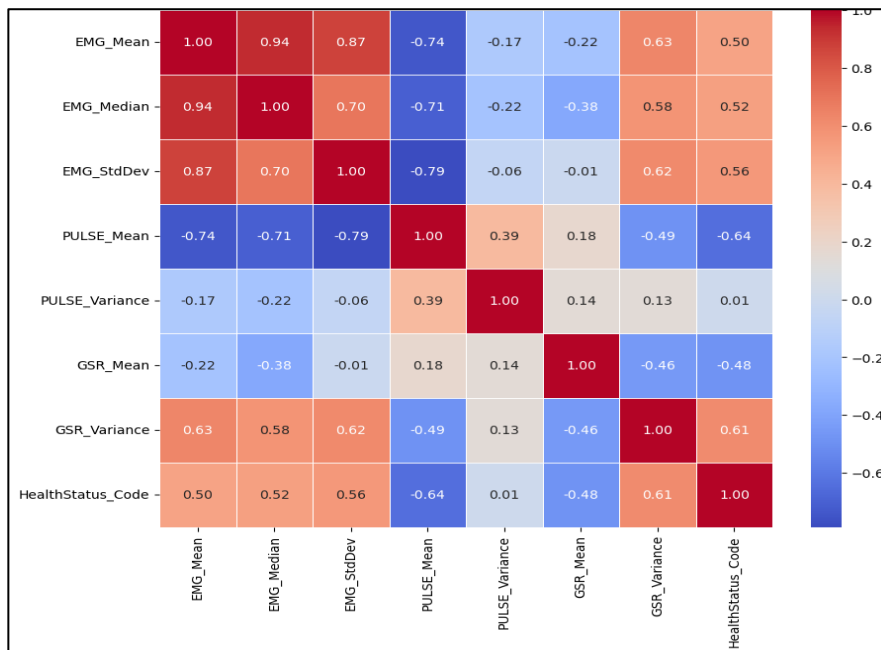


**Figure 16.** Correlation Matrix for Features and Health Status

If EMG\_Mean and PULSE\_Mean have  $r \approx 0.8$  in healthy individuals but  $r \approx 0.1$  in unhealthy subjects, it suggests that muscle activity and heart rate are no longer functioning together as expected in psychiatric risk. EMG\_Mean and GSR\_Mean have a correlation of 0.75, indicating a strong positive correlation (they tend to increase together). PULSE\_Mean and PULSE\_StdDev have a correlation of 0.8, indicating high correlation (patients with a high pulse rate also have high fluctuations in pulse). EMG\_Mean and PULSE\_StdDev have a correlation of -0.5, implying moderate negative correlation (when EMG\_Mean increases, PULSE\_StdDev tends to decrease). The correlation matrix helps to understand which features indicate abnormal responses in psychiatric risk.

The distribution of the subjects' GSR, EMG, and pulse measurements is shown in a box plot in Figure 17. It is possible to analyze the physiological signal levels based on this. A box plot showing the distribution of EMG, GSR, and pulse (heart rate) values highlights the characteristics of each parameter's fundamental tendency and variability. The IQR of EMG readings is between 150 and 250, with a center of 200. A number of outliers above 300 point to sporadic elevated EMG readings. With an IQR ranging from 350 to 450 and a median of about 400, GSR shows the highest values. Below 300, there are many outliers, which suggest that lower GSR responses vary. With values clustered between 80 and 100 and a median close to 90, Pulse exhibits the least amount of fluctuation. Both below 70 and above 110, there are several outliers. Overall, EMG has moderate dispersion with a noticeable high value, Pulse is the most stable, and GSR has the largest fluctuation. The physiological patterns illustrated by this box plot may aid in the diagnosis, observation, and comprehension of psychiatric risk.

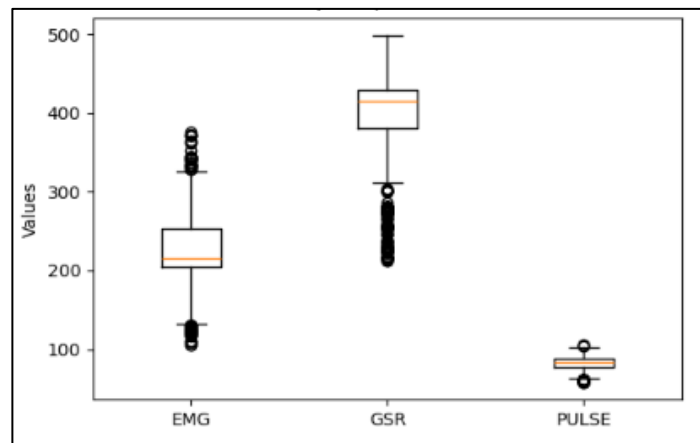


Figure 17. Distribution of the EMG, GSR and Pulse Measurements of a Subject

The excellent model accuracy implies that these biomarkers provide useful prediction data for spotting patterns linked to Psychiatric risk.

#### 4. Conclusion

The abnormal behavioral state causes individuals to sweat, feel agitated, and experience an increase in heartbeat due to physiological abnormalities. This study presents a framework using a machine learning model for individuals affected by Endosulfan spray in the regions of Karnataka State, India. All three models, namely Random Forest, XGBoost, and Neural Networks, achieved a sustainable classification accuracy of 97.92% using biosensor GSR, EMG, and pulse data. The real-time acquired features were validated for clinical significance ( $p < 0.05$ ) using a t-test. This study demonstrates consistent performance using statistical

analyses such as Kernel Density Estimation (KDE), correlation matrix, angle prediction, feature engineering, and heatmap statistics. Biosignals, which directly represent the neurological systems, help disabled individuals and their caregivers improve their quality of routine life. Furthermore, this study extends to the detection of behavioral symptoms, including those associated with schizophrenia.

## Acknowledgement

Authors are thankful to Sanidhya Skill Training Centre for Endosulfan victims, Ujire, of Karnataka State, India for their ethical support in data collection, and Pragathi Speciality Hospital, Puttur, India for medical expertise and validation of this study.

## Conflicts of Interest

The authors declare, there is no conflict of interest in regard to this research article.

## Funding Declarations

There was no external funding in this study.

## Contributor Roles Taxonomy (CRediT) Author Statement

Conceptualization & Methodology: Akshaya D. Shetty (A.D.S.), and Usha Desai (U.D.); Experimental Work: A.D.S.; Writing—Original Draft Preparation: A.D.S.; Writing—Review and Editing: U.D., and Akash Saxena (A.S.); Supervision: U.D., and A.S.

All authors have read and approved the final version of the manuscript.

## References

- [1] World Health Organization. (2025). Schizophrenia. World Health Organization. <https://www.who.int/news-room/fact-sheets/detail/schizophrenia>
- [2] Damiani, Stefano, Marco Cavicchioli, Cecilia Guiot, Alberto Donadeo, Andrea Scalabrini, Valentina Grecuzzo, Irma Bergamaschini, Umberto Provenzani, Pierluigi Politi, and Paolo Fusar-Poli. "The Noise in Our Brain: A Systematic Review and Meta-Analysis of Neuroimaging and Signal-Detection Studies on Source Monitoring in Psychosis." *Journal of psychiatric research* 169 (2024): 142-151.
- [3] Coutts, F., Koutsouleris, N., & McGuire, P. (2023). Psychotic Disorders as a Framework for Precision Psychiatry. *Nature Reviews Neurology*, 19(4), 221–234. <https://doi.org/10.1038/s41582-023-00779-1>.
- [4] Markiewicz, Renata, Agnieszka Markiewicz-Gospodarek, and Beata Dobrowolska. "Galvanic Skin Response Features in Psychiatry and Mental Disorders: A Narrative Review." *International journal of environmental research and public health* 19, no. 20 (2022): 13428. <https://doi.org/10.3390/ijerph192013428>

- [5] Khullar, Vikas, Raj Gaurang Tiwari, Ambuj Kumar Agarwal, and Soumi Dutta. "Physiological Signals Based Anxiety Detection Using Ensemble Machine Learning." In *Cyber Intelligence and Information Retrieval: Proceedings of CIIR 2021*, pp. 597-608. Singapore: Springer Singapore, 2021. [https://doi.org/10.1007/978-981-16-4284-5\\_53](https://doi.org/10.1007/978-981-16-4284-5_53)
- [6] Long, Nannan, Yongxiang Lei, Lianhua Peng, Ping Xu, and Ping Mao. "A Scoping Review on Monitoring Mental Health Using Smart Wearable Devices." *Math. Biosci. Eng* 19, no. 8 (2022): 7899-7919. <https://doi.org/10.3934/mbe.2022369>
- [7] Nakagome, Kazuyuki, Manabu Makinodan, Mitsuhiro Uratani, Masaki Kato, Norio Ozaki, Seiko Miyata, Kunihiro Iwamoto et al. "Feasibility of a Wrist-Worn Wearable Device for Estimating Mental Health Status in Patients with Mental Illness." *Frontiers in Psychiatry* 14 (2023): 1189765. <https://doi.org/10.3389/fpsy.2023.1189765>
- [8] Shehu, Harisu Abdullahi, Matt Oxner, Will N. Browne, and Hedwig Eisenbarth. "Prediction of Moment-By-Moment Heart Rate and Skin Conductance Changes in the Context of Varying Emotional Arousal." *Psychophysiology* 60, no. 9 (2023): e14303. <https://doi.org/10.1111/psyp.14303>
- [9] Nawawi, Nurfathin A., Rubita Sudirman, and Usman U. Sheikh. "Drowsiness Detection Using Galvanic Skin Response and Electro-Occulograph." In *Journal of Physics: Conference Series*, vol. 2622, no. 1, p. 012004. IOP Publishing, 2023. <https://doi.org/10.1088/1742-6596/2622/1/012004>
- [10] Amit, Guy, Yonatan Bilu, Tamar Sudry, Meytal Avgil Tsadok, Deena R. Zimmerman, Ravit Baruch, Nitsa Kasir, Pinchas Akiva, and Yair Sadaka. "Early Prediction of Autistic Spectrum Disorder Using Developmental Surveillance Data." *JAMA network open* 7, no. 1 (2024): e2351052. [doi.org/10.1001/jamanetworkopen.2023.51052](https://doi.org/10.1001/jamanetworkopen.2023.51052)
- [11] Cox, Olivia D., Ananya Munjal, William V. McCall, Brian J. Miller, Chris Baeken, and Peter B. Rosenquist. "A Review of Clinical Studies of Electrodermal Activity and Transcranial Magnetic Stimulation." *Psychiatry Research* 329 (2023): 115535. <https://doi.org/10.1016/j.psychres.2023.115535>
- [12] Ihmig, Frank R., Frank Neurohr-Parakenings, Sarah K. Schäfer, Johanna Lass-Hennemann, and Tanja Michael. "On-Line Anxiety Level Detection from Biosignals: Machine Learning Based on a Randomized Controlled Trial with Spider-Fearful Individuals." *Plos one* 15, no. 6 (2020): e0231517. <https://doi.org/10.1371/journal.pone.0231517>
- [13] Grabowski, Karol, Agnieszka Rynkiewicz, Amandine Lassalle, Simon Baron-Cohen, Björn Schuller, Nicholas Cummins, Alice Baird, Justyna Podgórska-Bednarz, Agata Pieniążek, and Izabela Łucka. "Emotional Expression in Psychiatric Conditions: New Technology for Clinicians." *Psychiatry and clinical neurosciences* 73, no. 2 (2019): 50-62. <https://doi.org/10.1111/pcn.12799>
- [14] Ding, Xinfang, Xinxin Yue, Rui Zheng, Cheng Bi, Dai Li, and Guizhong Yao. "Classifying Major Depression Patients and Healthy Controls Using EEG, Eye Tracking and Galvanic Skin Response Data." *Journal of affective Disorders* 251 (2019): 156-161. <https://doi.org/10.1016/j.jad.2019.03.058>

- [15] Sun, Xiao, Tao Hong, Changliang Li, and Fuji Ren. "Hybrid Spatiotemporal Models for Sentiment Classification Via Galvanic Skin Response." *Neurocomputing* 358 (2019): 385-400. <https://doi.org/10.1016/j.neucom.2019.05.061>
- [16] Domínguez-Jiménez, Juan Antonio, Kiara Coralia Campo-Landines, Juan C. Martínez-Santos, Enrique J. Delahoz, and Sonia H. Contreras-Ortiz. "A Machine Learning Model for Emotion Recognition from Physiological Signals." *Biomedical signal processing and control* 55 (2020): 101646. <https://doi.org/10.1016/j.bspc.2019.101646>
- [17] Horn, Mathilde, Thomas Fovet, Guillaume Vaiva, Pierre Thomas, Ali Amad, and Fabien d'Hondt. "Emotional Response in Depersonalization: A Systematic Review of Electrodermal Activity Studies." *Journal of affective disorders* 276 (2020): 877-882. <https://doi.org/10.1016/j.jad.2020.07.064>
- [18] Tawhid, Md Nurul Ahad, Siuly Siuly, and Hua Wang. "Diagnosis of Autism Spectrum Disorder from EEG Using a Time–Frequency Spectrogram Image-Based Approach." *Electronics Letters* 56, no. 25 (2020): 1372-1375. <https://doi.org/10.1049/el.2020.2646>
- [19] Desai, Usha, and Akshaya D. Shetty. "Electrodermal Activity (EDA) for Treatment of Neurological and Psychiatric Disorder Patients: A Review." In *2021 7th International Conference on Advanced Computing and Communication Systems (ICACCS)*, vol. 1, IEEE, 2021, 1424-1430. <https://doi.org/10.1109/ICACCS51430.2021.9441808>
- [20] Desai, U., Shetty, A. D., M, T., A, A. S., Nekar, G., & B, S. (2022). Detection of Anxiety in Psychiatric Patients using Physiological Signals. *2022 IEEE 19th India Council International Conference (INDICON)*, 1–5. <https://doi.org/10.1109/indicon56171.2022.10040142>
- [21] Kargarandehkordi, Ali, Shizhe Li, Kaiying Lin, Kristina T. Phillips, Roberto M. Benzo, and Peter Washington. "Fusing Wearable Biosensors with Artificial Intelligence for Mental Health Monitoring: A Systematic Review." *Biosensors* 15, no. 4 (2025): 202. <https://doi.org/10.3390/bios15040202>
- [22] Wang, Lin, Yubing Hu, Nan Jiang, and Ali K. Yetisen. "Biosensors for Psychiatric Biomarkers in Mental Health Monitoring." *Biosensors and Bioelectronics* 256 (2024): 116242. <https://doi.org/10.1016/j.bios.2024.116242>
- [23] Tettey-Engmann, Felix, Santosh Kumar Parupelli, Steven R. Bauer, Narayan Bhattarai, and Salil Desai. "Advances in Artificial Intelligence-Based Medical Devices for Healthcare Applications." *Biomedical Materials & Devices* (2025): 1-21. <https://doi.org/10.1007/s44174-025-00379-1>
- [24] Xing, Yantao, Yang Yang, Kaiyuan Yang, Albert Lu, Luyi Xing, Ken Mackie, and Feng Guo. "Intelligent Sensing Devices and Systems for Personalized Mental Health." *Med-x* 3, no. 1 (2025): 10. <https://doi.org/10.1007/s44258-025-00057-3>
- [25] Pillai, Renjith R., Sekar Kasi, and Dilip Diwakar. "Prevalence of Psychological Distress Among the Caregivers of an Endosulfan Disaster Victims in India: A Cross-Sectional Community-Based Study." *The Egyptian Journal of Neurology, Psychiatry and Neurosurgery* 59, no. 1 (2023): 78. <https://doi.org/10.1186/s41983-023-00678-8>